Measurement of the single polarization observables I^c and I^s in $\pi^0\eta$ photoproduction

E. Gutz
for the CBELSA/TAPS Collaboration

Helmholtz-Institut für Strahlen- und Kernphysik, Universität Bonn, Germany

Abstract. Meson photoproduction off the nucleon is a key tool in order to understand the structure of baryons and their excitation spectrum. Especially in the regime of high-lying resonances the photoproduction of multi-meson final states is of increasing importance, given that the cross sections for such processes exceed those for single-meson production. Additionally it gives a handle on sequential decays of such resonances via e.g. the $\Delta(1232)$ or the $S_{11}(1535)$ in the intermediate state. For a complete understanding of the processes involved, the measurement not only of unpolarized cross sections but also of polarization observables is mandatory. With the Crystal Barrel/TAPS experiment, located at the ELSA accelerator facility in Bonn, it was possible to determine such observables using a linearly polarized photon beam impinging on a liquid hydrogen target. The beam asymmetries I^c and I^s are presented for the reaction $\vec{\gamma}p \rightarrow p\pi^0\eta$. The latter is a feature exclusive to the acoplanar kinematics of multi-meson final states and has been measured for the first time.

Keywords: Photoproduction, pseudoscalar mesons, polarization observables
PACS: 13.60.-r, 13.60.Le, 13.88.+e

INTRODUCTION

The photoproduction of pseudoscalar meson pairs off the nucleon yields a great potential for gaining further insight in the field of baryons and their properties. At present, much of our understanding of the excitation spectrum of the nucleon is based on constituent quark models [1]. While in general quite sucessful in the description of the baryon spectrum, these models exhibit certain shortcomings, most prominently the prediction of an abundance of states with masses above 1.8 GeV for which little to no experimental evidence exists from πN scattering [2] (*missing resonances*). The photoproduction of meson pairs not only avoids the experimental bias of πN couplings, but also allows for the study of sequential decays of such high lying resonances. The reaction $\gamma p \rightarrow p\pi^0\eta$ is particularly attractive in this context since the isoscalar η allows for the distinct study of excited Δ states via their $\Delta\eta$ decay. Accordingly, the investigation of this reaction has gained in importance over the past few years, both experimentally and theoretically. Unpolarized total and differential cross sections have been measured by various experiments [3, 4, 5] as well as the beam asymmetry Σ [5, 6]. From the theoretical side, attempts to treat the $\Delta(1700)D_{33}$ as resonance that is dynamically generated from Δ-η interactions [7] have been made as well as attempts to understand the rapidly rising cross section [8] by formation of intermediate resonances. A coupled-channel partial wave analysis within the Bonn-Gatchina framework (BnGa-PWA) [9] suggests the formation of, among others, the established (three star) $\Delta(1920)P_{33}$ and a not-well-known (one-star) $\Delta(1940)D_{33}$ resonance in this reaction [4]. These two resonances seem to form a further parity doublet. Such parity doublets have been related to a restoration of chiral symmetry at high baryon excitation masses [10].

Experimentally, the main key to a good understanding of the baryon spectrum is the measurement of a complete set of observables for a multitude of final states, only one of which is the unpolarized cross section. While in single-meson production out of a total of 16 accessible observables a well chosen set of 8 measurements suffices for a model-independent, unambiguous partial wave analysis (*complete experiment*, [11]), additional degrees of freedom in two-meson production lead to a total of 64 possible observables. Here identities lead to a set of 15 independent measurements which need to be taken out for a complete experiment [12].

These additional degrees of freedom arise from the fact that two-meson photoproduction is not - like two-body reactions - restricted to a single plane, but two planes, a reaction and a decay plane enclosing an angle ϕ^*, occur as seen in Fig. 2a. As a consequence, here polarization asymmetries can also occur if e.g. only the target is longitudinally polarized or if only the beam is circularly polarized, which is not possible in single-meson production. The first measurements of such asymmetries in double-pion production using circularly polarized photons [13] have demonstrated

their significant model sensitivity and revealed serious deficiencies of most available models.

In the case of linearly polarized photons impinging on an unpolarized target two polarization observables I^s and I^c occur, for which so far no data has been published in any channel. The latter corresponds to the polarization observable Σ if the dependence on the angle ϕ^* is integrated out. The cross section can be written in the form

$$\frac{d\sigma}{d\Omega} = \left(\frac{d\sigma}{d\Omega}\right)_0 \left\{1 + \delta_l[I^s \sin(2\phi) + I^c \cos(2\phi)]\right\}, \tag{1}$$

[12] where $\left(\frac{d\sigma}{d\Omega}\right)_0$ is the unpolarized cross section, δ_l the degree of linear photon polarization, and ϕ the azimuthal angle of the reaction plane with respect to the normal on the polarization plane. The occuring observables I^s (I^c) can be expressed as the imaginary (real) part of a linear combination of bilinears formed from the helicity or transversity amplitudes that describe the process. They are therefore not only particularly sensitive to interference effects, but also to the relative phases of the amplitudes, which allows a much more precise extraction of resonance parameters than by unpolarized data alone.

EXPERIMENTAL SETUP
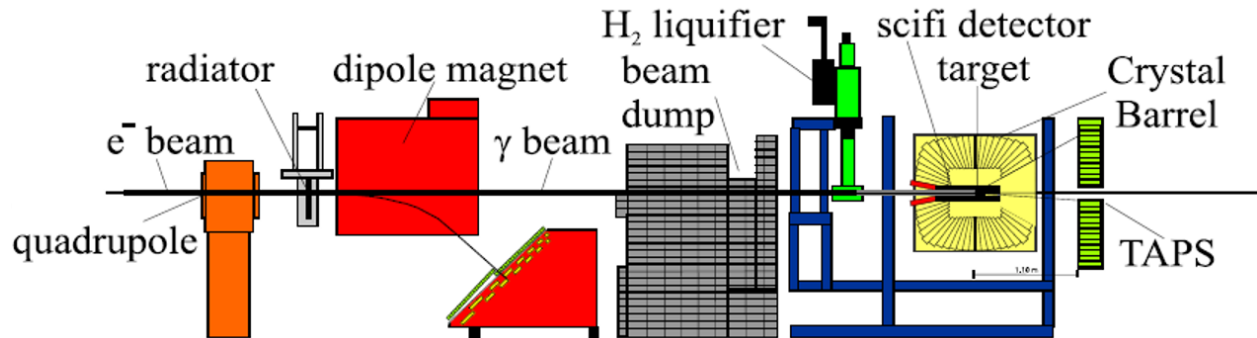
FIGURE 1. Setup of the CBELSA/TAPS experiment. The primary electron beam enters from the left. For details see text.

The data presented were obtained by the CBELSA/TAPS experiment located at the ELectron Stretcher Accelerator (ELSA) [14] in Bonn. The experimental setup is shown in Fig. 1. The primary electron beam extracted from ELSA enters from the left with an energy of 3.2 GeV. The linearly polarized photons are produced via coherent bremsstrahlung off a diamond radiator. Electrons undergoing the bremsstrahlung process are then momentum analyzed using a tagging spectrometer consisting of a dipole magnet and a scintillator based detection system. The associated photons travel further along the beamline, impinging on a 5 cm long liquid hydrogen target [15] in the center of the Crystal Barrel calorimeter [16]. The Crystal Barrel consists of 1290 CsI(Tl) crystals in a ϕ-symmetric setup covering the polar angle from 30° to 168° and the full azimuthal range. In forward direction the TAPS calorimeter [17], comprising 528 BaF$_2$ modules in a forward wall setup, covers the polar angle down to 5°. In front of each of these modules a 5 mm thick plastic scintillator allows for the identification of charged particles. An additional means for charge identification, a three-layer scintillating fibre detector [18], surrounds the reaction target, covering the angular range of the Crystal Barrel calorimeter. For further details on the experimental setup, see [19].

DATA ANALYSIS

For this analysis, two datasets were considered, both obtained with a primary electron energy of 3.2 GeV. The maximum degrees of polarization for these datasets were 49.2% at $E_\gamma = 1300$ MeV (setting A) and 38.7% at 1600 MeV (setting B), respectively. The systematic error of the polarization was determined to be $\Delta P \leq 0.02$ [20]. To guarantee a sufficiently high degree of polarization for the data analyzed, the datasets were subdivided into three energy bins, $W = 1706 \pm 64$ MeV, 1834 ± 64 MeV, and 1946 ± 48 MeV respectively, where the low energy range consists solely of data taken with the polarization setting A, the high energy range of data taken with setting B. For the intermediate
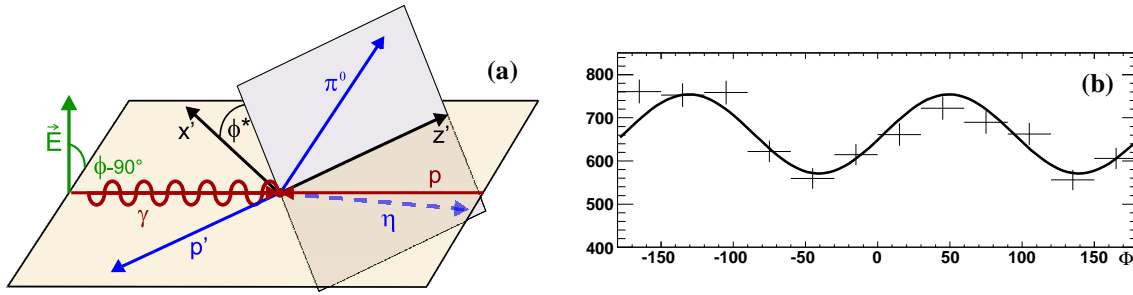
FIGURE 2. (a) Angle definitions in the center-of-momentum frame. ϕ^* is the angle between the reaction plane defined by the incoming photon and recoiling particle p' and the decay plane of two final state particles. (b) Example of a measured ϕ-distribution. Shown is the ϕ-distribution of the final state proton in the region $60° \leq \phi^* \leq 120°$ for events in the energy range $W = 1834 \pm 64$ MeV (y-axis with suppressed-zero scale).

energy range, both datasets were combined.

The datasample was selected for events with five distinct calorimeter hits since only the 2γ decays of the final state mesons were considered. To avoid possible systematic effects due to scintillator inefficiencies, charge information was not used to identify the proton. Events were retained if one or more combinations of four out of the five clusters were compatible with a π^0 and an η, meaning the according two-particle invariant masses agreed with the respective meson masses within 4σ. To ascertain the proton, the direction of the fifth cluster had to agree with the missing momentum determined from the two mesons within $10°$ in ϕ and, taking the angular resolution of the calorimeters into account, within $5°$ in θ for TAPS and $15°$ for the Crystal Barrel, respectively. Also, the missing mass of the meson system had to be consistent with the proton mass within 4σ.

After this preselection, the data was subjected to a kinematic fit [21] imposing energy and momentum conservation, assuming that the interaction took place in the target center. Events were retained if they exceeded a probability (CL) of 8% for the $\gamma p \rightarrow p\pi^0\gamma\gamma$ two-constraint hypothesis and of 6% for the $\gamma p \rightarrow p\pi^0\eta$ three-constraint hypothesis, respectively. Events compatible with CL > 1% for the $\gamma p \rightarrow p\pi^0\pi^0$ hypothesis were rejected. The proton direction resulting from the fit had to agree with the direction of the proton determined in the preselection within $20°$. This led to a final event sample containing a total of 65431 $p\pi^0\eta$ events with a maximum background contamination of 1%. To extract the polarization observables defined in Eq. (1), the ϕ-distributions of the final state particles were fit with the expression

$$f(\phi) = A + P[B\sin(2\phi) + C\cos(2\phi)], \qquad (2)$$

with P being the polarization determined for each event individually and later averaged for each fitted bin. Fig. 2b shows an example of an according distribution. The effect of both beam asymmetries is clearly visible in the distinct superposition of a $\cos(2\phi)$- (I^c) and a $\sin(2\phi)$-modulation (I^s).

RESULTS

Figures 3 - 5 show the beam asymmetries I^s (top) and I^c (bottom), extracted from the fits to the ϕ-distributions as described above for the three energy ranges (left to right) $W = 1706 \pm 64$ MeV, 1834 ± 64 MeV, and 1946 ± 48 MeV [22]. Depicted as filled symbols are the asymmetries obtained when treating the proton (Fig. 3), π^0 (Fig. 4), and η (Fig. 5) as recoiling particle (see Fig. 2a). The open symbols are obtained by performing the transition $\phi^* \rightarrow 2\pi - \phi^*$, which is equivalent to a mirror operation with respect to the reaction plane, and in the case of I^s changing the sign of the asymmetry. In case of linear polarization such a mirror operation leads to the transition $\phi \rightarrow 2\pi - \phi$ and because of $\sin(2 \cdot (2\pi - \phi)) = -\sin(2\phi)$ $(\cos(2 \cdot (2\pi - \phi)) = -\cos(2\phi))$ to $I^s(2\pi - \phi^*) \rightarrow -I^s(\phi^*)$ $(I^c(2\pi - \phi^*) \rightarrow I^c(\phi^*))$. These symmetry constraints are well fulfilled within statistics, indicating comparably small systematic uncertainties. An estimate of the systematic uncertainties is given by the bar graphs below the asymmetries in Figures 3 - 5. They have been determined by once applying a 2-dimensional acceptance and efficiency correction as function of the variables ϕ and ϕ^* for each energy bin and in addition, since effects due to the contributing physics amplitudes have to be considered, using the result of the PWA discussed below to study the acceptance and efficiency. The systematic error shown reflects the maximal effect determined by these methods.

The data has been incorporated in the BnGa multi-channel partial wave analysis which gives the opportunity to test
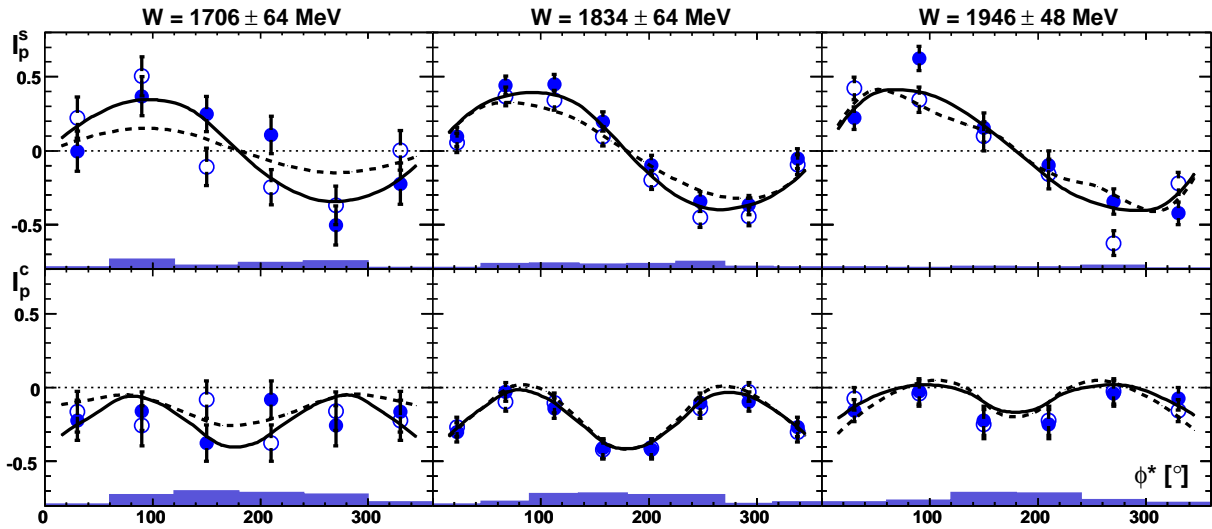
FIGURE 3. Measured beam asymmetries I^s (top) and I^c (bottom) in the reaction $\vec{\gamma}p \to p\pi^0\eta$ [22], treating the proton as recoiling particle. Left to right: CMS energy ranges 1706 ± 64 MeV, 1834 ± 64 MeV, 1946 ± 48 MeV. Filled symbols: $I^s(\phi^*)$ $(I^c(\phi^*))$, open symbols: $-I^s(2\pi - \phi^*)$ $(I^c(2\pi - \phi^*))$. Solid curve: Full BnGa-PWA fit, dashed curve: BnGa-PWA fit excluding $3/2^-$-wave. Histograms below: Estimate of systematic errors due to acceptance and efficiency.
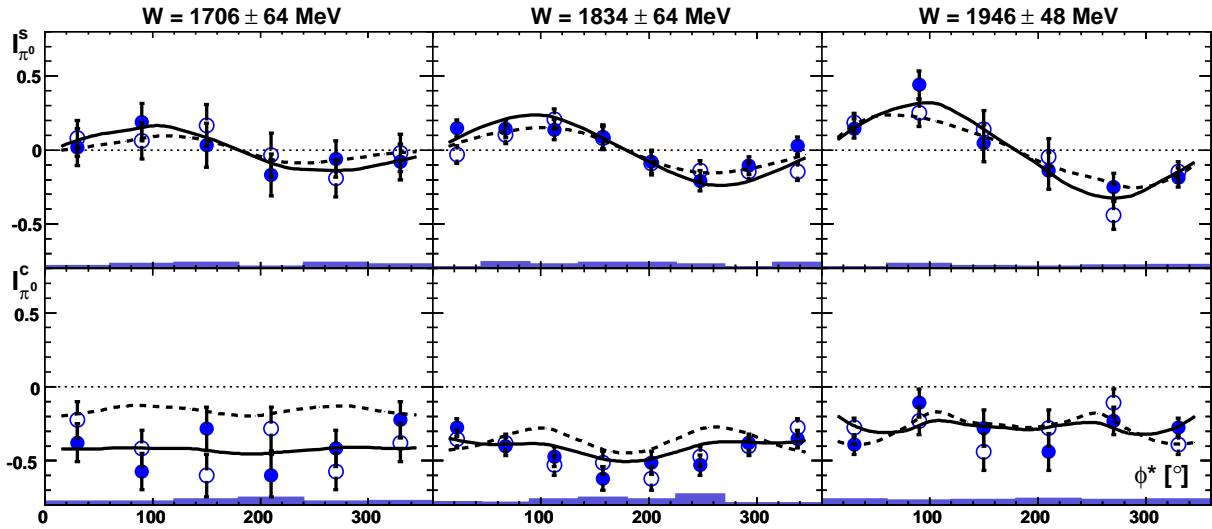
FIGURE 4. Measured beam asymmetries I^s (top) and I^c (bottom) in the reaction $\vec{\gamma}p \to p\pi^0\eta$ [22], treating the π^0 as recoiling particle. Notation as Fig. 3.

its sensitivity to certain partial wave contributions. A previous fit [4], including data on the reaction $\gamma p \to p\pi^0\eta$ but without information on I^s and I^c presented here, had claimed evidence for contributions from negative- and positive-parity Δ resonances with spin $J = 3/2$, namely the poorly established $\Delta(1940)D_{33}$ along with the well established $\Delta(1700)D_{33}$, $\Delta(1600)P_{33}$, and $\Delta(1920)P_{33}$. The result of a new fit including I^s and I^c is shown in Figs. 3 - 5 as solid curves. Removing the couplings of the $3/2^+$-wave to $p\pi^0\eta$ (which provides a small fraction of the total cross section only) results in a fit to I^s and I^c which is still acceptable; larger discrepancies are only observed in differential cross sections. However, removing the $3/2^-$-wave which includes the above mentioned resonances $\Delta(1700)$ and $\Delta(1940)$ leads to fits, shown in Figs. 3 - 5 as dashed curves, in which significant discrepancies are observed.
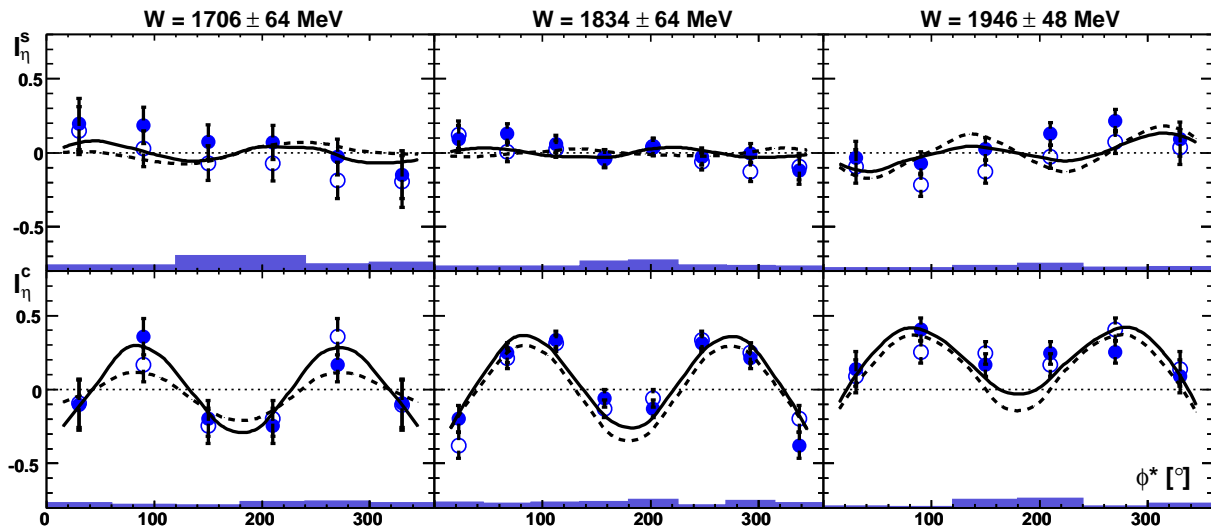
FIGURE 5. Measured beam asymmetries I^s (top) and I^c (bottom) in the reaction $\vec{\gamma}p \to p\pi^0\eta$ [22], treating the η as recoiling particle. Notation as Fig. 3.

SUMMARY AND CONCLUSIONS

The two beam asymmetries accessible in two-meson production using linearly polarized photons and an unpolarized target, I^c and I^s have been extracted for the reaction $\vec{\gamma}p \to p\pi^0\eta$ from data taken with the CBELSA/TAPS experiment. While the former would correspond to the beam asymmetry Σ if the ϕ^*-dependence is integrated out, no information about the latter asymmetry has been available as of yet. Fits within the framework of the BnGa-PWA demonstrate that I^s and I^c carry significant information on the contributing partial waves. This observation underlines the importance of polarization observables in general and demonstrates the significance of I^s and I^c as new polarization observables in particular.

REFERENCES

1. S. Capstick, W. Roberts, Prog. Part. Nucl. Phys. **45**, 241 (2000); U. Löring *et al.*, Eur. Phys. J. A **10**, 309, 395, 447 (2001).
2. C. Amsler *et al.*, Phys. Lett. B **667**, 1, (2008) .
3. T. Nakabayashi *et al.*, Phys. Rev. C **74**, 035202 (2006); V.L. Kashevarov *et al.*, Eur. Phys. J. A **42**, 141 (2009).
4. I. Horn *et al.*, Phys. Rev. Lett. **101**, 202002 (2008); I. Horn *et al.*, Eur. Phys. J. A **38**, 173 (2008).
5. J. Ajaka *et al.*, Phys. Rev. Lett. **100**, 052003 (2008).
6. E. Gutz, V. Sokhoyan, H. van Pee *et al.*, Eur. Phys. J. A **35**, 291 (2008).
7. M. Döring, E. Oset, D. Strottman, Phys. Rev. C **73**, 045209 (2006).
8. A. Fix, M. Ostrick, L. Tiator, Eur. Phys. J. A **36**, 61 (2008).
9. A.V. Anisovich *et al.*, Eur. Phys. J. A **24**, 111 (2005); A.V. Anisovich *et al.*, *ibid.* **34**, 243 (2007).
10. L. Y. Glozman, Phys. Lett. B **475**, 329 (2000).
11. W.-T. Chiang, F. Tabakin, Phys. Rev. C **55**, 2054 (1997).
12. W. Roberts, T. Oed, Phys. Rev. C **71**, 055201 (2005).
13. S. Strauch *et al.*, Phys. Rev. Lett. **95**, 162003 (2005); D. Krambrich *et al.*, *ibid.*. **103**, 052002 (2009).
14. W. Hillert, Eur. Phys. J. A **28**, 139 (2006).
15. B. Kopf, Ph.D. thesis, Dresden (2002).
16. E. Aker *et al.*, Nucl. Inst. and Meth. A **321**, 69 (1992).
17. R. Novotny, IEEE Trans. Nucl. Sci. **NS-38**, 379 (1991); A.R. Gabler *et al.*, Nucl. Inst. and Meth. A **346**, 168 (1994).
18. G. Suft *et al.*, Nucl. Inst. and Meth. A **538**, 416 (2005).
19. D. Elsner *et al.*, Eur. Phys. J. A **33** (2), 147 (2007).
20. D. Elsner *et al.*, Eur. Phys. J. A **39** (3), 373 (2009).
21. H. van Pee *et al.*, Eur. Phys. J. A **31**, 61 (2007).
22. E. Gutz, V. Sokhoyan, H. van Pee *et al.*, arXiv:0912.2632 [nucl-ex], submitted for publication.